

Efficient DMFT-simulation of the Holstein-Hubbard Model

Philipp Werner and Andrew J. Millis
Columbia University, 538 West, 120th Street, New York, NY 10027, USA
(Dated: May 26, 2019)

We present a method for solving impurity models with electron-phonon coupling, which treats the phonons efficiently and without approximations. The algorithm is applied to the Holstein-Hubbard model in the dynamical mean field description, where it allows access to strong interactions, very low temperatures and arbitrary fillings. We show, contrary to widely-held assumptions, that in strongly correlated materials the phonon contribution to the self-energy is not well described by Migdal-Eliashberg theory. In particular, phonons do not make a simple additive contribution, appearing at or below the phonon frequency.

PACS numbers: 71.10.Fd, 71.28.+d, 71.30.+h, 71.38.k

Electron-lattice interactions play a fundamental role in the physics of metals. In conventional (“weakly correlated”) materials such as Al or MgB₂, phonons are the dominant source of inelastic scattering and provide the pair binding which leads to superconductivity. In these materials, physical understanding is greatly aided by the Migdal-Eliashberg theory, which justifies the use of density functional band theory methods to estimate the electron-phonon coupling constants and perturbative methods to estimate electron mass renormalizations, lifetimes and pairing strengths. A key result of the Migdal-Eliashberg theory is that the effect of the electrons on the phonons is a renormalization of the phonon oscillator frequency ω_0 , while the effect of the phonons on the electrons is an increase in the electron effective mass. The mass increase “turns on” at frequencies below the renormalized phonon frequency.

In unconventional (“strongly correlated”) materials such as the high temperature superconductors [1], the fullerenes [2, 3], or the colossal magnetoresistance rare-earth manganites [4, 5] the situation is less clear. Many experiments suggest that electron-phonon effects are important. For example, in high T_c superconductors changes attributed to the electron-phonon coupling are observed in the electronic dispersion [1] at energies of the order of typical optical phonon frequencies. However, there is as yet no clear theoretical basis for interpreting these or related data in strongly correlated materials. While there has been extensive and important work on static properties of models involving electron-electron and electron-phonon coupling [6, 7], on Fermi-liquid and effective field theory based approaches [8, 9], and on the polaron problem (one electron in a correlated background) [10, 11] less is known about the dynamical consequences of the electron-phonon interaction in strongly correlated materials.

A way forward is provided by dynamical mean field theory (DMFT), a powerful, non-perturbative tool to study the properties of strongly correlated systems, which has provided considerable insight into the correlation induced metal-insulator (Mott) transition [12].

Progress in using dynamical mean field methods to study phonons coupled to strongly correlated electrons [13, 14, 15, 16] has been hampered by the mismatch in energy scales between the electronic and lattice parts of the problem and by the difficulty of providing a quantitative treatment of the low temperature properties of strongly correlated materials even in the absence of electron-phonon coupling. Phase diagrams and the dc limit of the mass enhancement have been computed, but while a few spectra have been presented a systematic understanding that will allow comparison to experiment seems not yet to exist. In this paper we introduce a new method which resolves these problems for the Holstein-Hubbard model. It allows the DMFT simulation of important classes of models at essentially the same computational expense as the corresponding models without coupling to phonons.

We consider the Holstein-Hubbard Hamiltonian

$$H = - \sum_{i,\delta,\sigma} t(\delta) c_{i+\delta,\sigma}^\dagger c_{i,\sigma} + \sum_i U n_{i,\uparrow} n_{i,\downarrow} - \mu(n_{i,\uparrow} + n_{i,\downarrow}) + \lambda \sum_i (b_i^\dagger + b_i)(n_{i,\uparrow} + n_{i,\downarrow} - 1) + \omega_0 \sum_i b_i^\dagger b_i. \quad (1)$$

Here, U denotes the on-site repulsion, μ the chemical potential of the electrons with creation operators c_σ^\dagger and density operators n_σ , b^\dagger the creation operator for Einstein phonons of frequency ω_0 , and the electron-phonon coupling is λ .

The single-site DMFT approximation [12] reduces the problem to the self-consistent solution of a quantum impurity model specified by the Hamiltonian $H_{\text{QI}} = H_{\text{loc}} + H_{\text{hyb}} + H_{\text{bath}}$. Here, the local term is

$$H_{\text{loc}} = -\mu(n_\uparrow + n_\downarrow) + U n_\uparrow n_\downarrow + \lambda(n_\uparrow + n_\downarrow - 1)(b^\dagger + b) + \omega_0 b^\dagger b, \quad (2)$$

and the impurity-bath mixing and bath Hamiltonians are $H_{\text{hyb}} = \sum_{p,\sigma} (V_{p,\sigma} c_\sigma^\dagger a_{p,\sigma} + V_{p,\sigma}^* c_\sigma a_{p,\sigma}^\dagger)$ and $H_{\text{bath}} = \sum_{p,\sigma} \epsilon_p a_{p,\sigma}^\dagger a_{p,\sigma}$. The parameters $V_{p,\sigma}$ are determined by a self-consistency equation.

In the absence of electron-phonon coupling, H_{loc} has a small Hilbert space (in the present example four

states) and one energy scale (U). Adding an electron-phonon coupling introduces a new energy scale, the phonon frequency ω_0 , and requires keeping track of the bosonic sector of the Hilbert space (with an infinite number of states). Previous approaches to the problem have involved either treating the bosons semiclassically [13, 17, 18] or simply truncating the boson Hilbert space, retaining only a finite number of boson states [14, 15, 16]. The semiclassical approach cannot account for quantal phonon effects such as electronic mass renormalization or superconductivity, while treating even a truncated boson Hilbert space directly is computationally expensive.

In Refs. [19, 20] we have shown that the stochastic sampling of a diagrammatic expansion of the partition function in powers of the impurity-bath hybridization term H_{hyb} leads to a highly efficient [21] impurity solver for purely electronic models. After tracing out the bath states $a_{p,\sigma}$, the weight of a Monte Carlo configuration corresponding to a perturbation order n (n creation operators $c_\sigma^\dagger(\tau_\sigma)$ and n annihilation operators $c_\sigma(\tau'_\sigma)$) can be expressed as

$$w(\{O_i(\tau_i)\}) = \text{Tr}_c \left\langle T_\tau e^{-\int_0^\beta d\tau H_{\text{loc}}(\tau)} O_{2n}(\tau_{2n}) \dots \right. \\ \left. \dots O_2(\tau_2) O_1(\tau_1) \right\rangle_b d\tau_1 \dots d\tau_{2n} \prod_\sigma (\det M_\sigma^{-1}) s_\sigma, \quad (3)$$

with $O_i(\tau_i)$ the (time ordered) creation and annihilation operators for spin up or down electrons on the impurity site. The matrix elements $(M_\sigma^{-1})_{i,j} = F_\sigma(\tau'_{\sigma,i} - \tau_{\sigma,j})$ are determined by the hybridizations $V_{p,\sigma}$ through the hybridization functions $F_\sigma(-i\omega_n) = \sum_p \frac{|V_{p,\sigma}|^2}{i\omega_n - \epsilon_p}$, as explained in Ref. [20]. The sign s_σ is 1 if the σ -spin operator with the lowest time argument is a creation operator and -1 otherwise.

The key idea of our approach is to use a Lang-Firsov [22] transformation to evaluate $\langle \dots \rangle_b$. Defining operators $X = (b^\dagger + b)/\sqrt{2}$ and $P = (b^\dagger - b)/i\sqrt{2}$, the unitary transformation specified by $e^{iP X_0}$ shifts X by $X_0 = (\sqrt{2}\lambda/\omega_0)(n_\uparrow + n_\downarrow - 1)$ so that

$$\tilde{H}_{\text{loc}} = e^{iP X_0} H_{\text{loc}} e^{-iP X_0} \\ = -\tilde{\mu}(\tilde{n}_\uparrow + \tilde{n}_\downarrow) + \tilde{U}\tilde{n}_\uparrow\tilde{n}_\downarrow + \frac{\omega_0}{2}(X^2 + P^2) \quad (4)$$

has no explicit electron-phonon coupling. \tilde{H}_{loc} is of the Hubbard form but with modified chemical potential and interaction strength: $\tilde{\mu} = \mu - \lambda^2/\omega_0$, $\tilde{U} = U - 2\lambda^2/\omega_0$. Also, the electron creation and annihilation operators are transformed according to $\tilde{c}_\sigma^\dagger = e^{\frac{\lambda}{\omega_0}(b^\dagger - b)} c_\sigma^\dagger$ and $\tilde{c}_\sigma = e^{-\frac{\lambda}{\omega_0}(b^\dagger - b)} c_\sigma$. The phonon contribution w_b to the weight (3) is $w_b(\{O_i(\tau_i)\}) = \langle e^{s_{2n}A(\tau_{2n})} \dots e^{s_1A(\tau_1)} \rangle_b$ with $0 \leq \tau_1 < \dots < \tau_{2n} < \beta$, $s_i = 1$ (-1) if the n^{th} operator is a creation (annihilation) operator and $A(\tau) = \frac{\lambda}{\omega_0}(e^{\omega_0\tau}b^\dagger - e^{-\omega_0\tau}b)$. This expectation value,

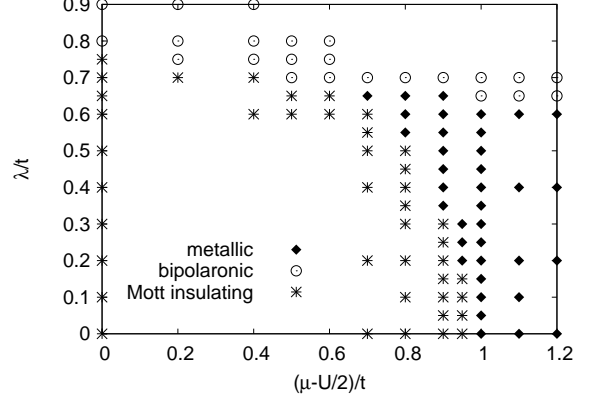


FIG. 1: Phase diagram for $\beta t = 50$, $U/t = 6$ in the plane of chemical potential μ and phonon coupling strength λ . Half-filling corresponds to $\mu = U/2$.

taken in the thermal state of free bosons, evaluates to

$$w_b(\{O_i(\tau_i)\}) = \exp \left[-\frac{\lambda^2/\omega_0^2}{e^{\beta\omega_0} + 1} \left(n(e^{\beta\omega_0} + 1) \right. \right. \\ \left. \left. + \sum_{2n \geq i > j \geq 1} s_i s_j \{ e^{\omega_0(\beta - (\tau_i - \tau_j))} + e^{\omega_0(\tau_i - \tau_j)} \} \right) \right], \quad (5)$$

and the weight (3) becomes the product

$$w(\{O_i(\tau_i)\}) = w_b(\{O_i(\tau_i)\}) \tilde{w}_{\text{Hubbard}}(\{O_i(\tau_i)\}), \quad (6)$$

where $\tilde{w}_{\text{Hubbard}}$ is the weight of a corresponding configuration in the Hubbard impurity model (without phonons, but modified parameters \tilde{U} and $\tilde{\mu}$). The Holstein-Hubbard model can thus be simulated without truncation at an expense comparable to the Hubbard model.

We have applied the method to the Holstein-Hubbard model with a semi-circular density of states of bandwidth $4t$ and $\omega_0/t = 0.2$. The correctness of our approach has been verified by comparison to previously obtained results at half-filling. Our low temperature ($\beta t = 400$) phase diagram as well as the quasi-particle weights are in very good agreement with those computed by NRG [14]. These and other data will be published elsewhere.

Figure 1 shows the phase diagram at $U/t = 6$ in the space of chemical potential and phonon coupling. If the chemical potential is increased at fixed electron-phonon coupling, a transition to a metal occurs. The critical chemical potential decreases as the electron-phonon coupling is increased. This behavior is physically expected: increasing the phonon coupling reduces the effective interaction \tilde{U} and so the magnitude of the insulating gap. We have confirmed this by analysis of the Green function. Our finding appears to contradict Ref. [15] which reported that the electron-phonon coupling stabilizes the insulating state. We believe the apparent difference arises from a choice of convention: the authors of Ref. [15] couple the phonons to the total density n , which implies

a static displacement of the phonon field (proportional to λn). This in turn leads to a static term in the electronic Hamiltonian which is equivalent to a shift in chemical potential. We couple the phonons to the difference in density from the half filled value, so that this shift (which we do not believe to be physically relevant) is not present at half filling. The transition driven by increasing λ at fixed μ is to a bipolaronic phase at incommensurate density and appears to be first order with a region of phase separation between the metal and the bipolaronic insulator. We do find, in agreement with the results of Ref. [15], that at the chemical potential driven transition the electronic compressibility $\partial n / \partial \mu|_\lambda$ increases with phonon coupling strength (for $\beta t = 50$ about a factor of 4 from $\lambda = 0$ to $\lambda = 0.6t$).

We now turn to our principal new results concerning the frequency dependence of the electron self energy. For orientation we note that in weakly correlated materials the conduction-band electrons renormalize the phonon propagator D from its bare value D_0 according to the RPA (ladder) result $D^{-1} = D_0^{-1} - \lambda^2 \chi_0$ with χ_0 the bare (unrenormalized by phonons) electronic density-density correlation function. The Migdal-Eliashberg approximation also implies that the local density-density correlator χ is given by

$$\chi(\Omega) = \chi_0(\Omega) / (1 - \lambda^2 D_0(\Omega) \chi_0(|\Omega|)). \quad (7)$$

The electron self energy is given in frequency space by the convolution $\Sigma = \lambda^2 G_0 * D$. It is convenient to present results as the Matsubara axis mass renormalization factor $r(i\omega_n) = -\Im m \Sigma(i\omega_n) / i\omega_n$. According to Migdal-Eliashberg theory, the effect of the electron-phonon coupling is to add to the purely electronic $r(i\omega_n)$ a term approximately of the form

$$r_{ME}(i\omega_n) = (2\lambda^2 N_0 / \omega_n) \arctan(\omega_n / \omega_0^{\text{ren}}) \quad (8)$$

with N_0 the Fermi surface density of states (in our case $\approx 1/2\pi t$). The zero frequency limit gives the electron-phonon contribution to the Fermi surface mass enhancement $m_{ME}^* / m = 2\lambda^2 N_0 / \omega_0^{\text{ren}}$ and r_{ME} drops to about half of its zero frequency value around $2\omega_0^{\text{ren}}$.

The upper panel of Fig. 2 compares the density-density correlation function computed from Eq. (7) to $\chi(\tau)$ measured in our QMC simulations, for $U = 0$ and several values of λ . Good agreement is seen; the small shift of λ required to match the $\lambda = 0.3$ QMC data ($\lambda_{EM} \approx 0.275$) is a beyond-Migdal effect arising from the small but non-vanishing effect of the electron self energy on χ_0 . The increase of $\chi(\tau)$ with λ shows the phonon character of the low frequency electronic correlations. In particular the decay constant characterizing the approximately exponential time decay observed for stronger couplings gives the renormalized phonon frequency ω_0^{ren} , while in the regimes where there is no clear evidence of exponential

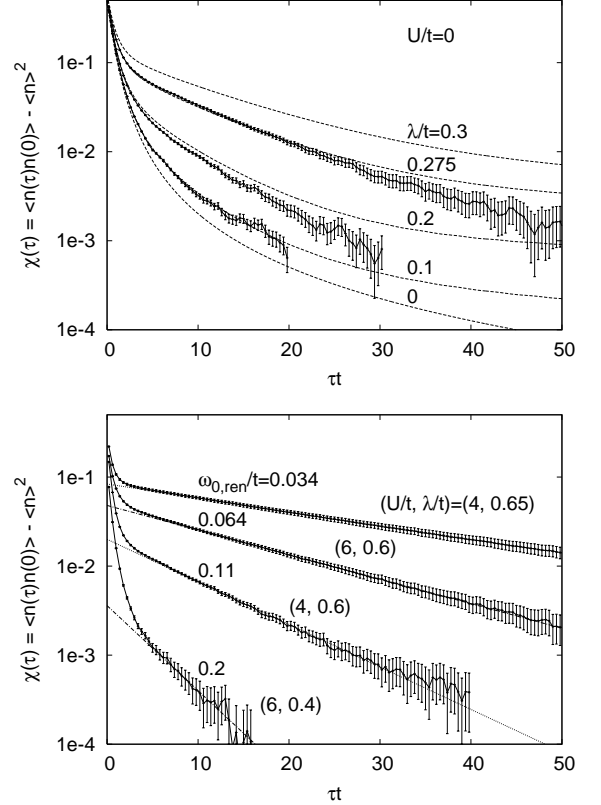


FIG. 2: Upper panel: $U = 0$ and $n = 1$. Dashed lines show $\chi(\tau)$ obtained from the Migdal-Eliashberg approximation (Eq. (7)) for indicated phonon couplings. Solid lines with $1-\sigma$ error bars show the QMC results at $\beta t = 400$. From bottom to top, the numerical data correspond to $\lambda/t = 0.1, 0.2$, and 0.3 . Lower panel: correlation functions for the interacting model at $U/t = 4$ and half-filling ($\lambda/t = 0.6, 0.65$) and in the doped Mott insulator at $U/t = 6$, $(\mu - U/2)/t = 1.2$ ($\lambda/t = 0.4, 0.6$). The renormalized phonon frequency ω_0^{ren} extracted from the exponential decay is also shown.

decay the phonon frequency is not significantly renormalized. For $U > 0$ the computed $\chi(\tau)$, shown in the lower panel of Fig. 2, is also seen to exhibit an exponential decay, from which we estimate ω_0^{ren} .

A phonon-related feature is not easily visible in the calculated self energies. Figure 3 presents our results as a comparison of the difference $\Delta r = -\Im m (\Sigma(\lambda, \delta, \omega_n) - \Sigma(0, \delta, \omega_n)) / \omega_n$ to Eq. (8), with $\Sigma(\lambda, \delta, \omega_n)$ denoting the self-energy for phonon coupling strength λ and doping per spin $\delta = n_\sigma - 0.5$. Previous work by one of us and by other groups [8, 13] had argued on the basis of Fermi liquid theory that the effect of phonons on correlated systems should be similar to that in uncorrelated systems, but with renormalized couplings. This is clearly seen to be inconsistent with our data. For the half filled model Δr is negative except for $\lambda/t = 0.65$ (very close to the bipolaronic phase): in other words the main effect of phonons is a decrease of

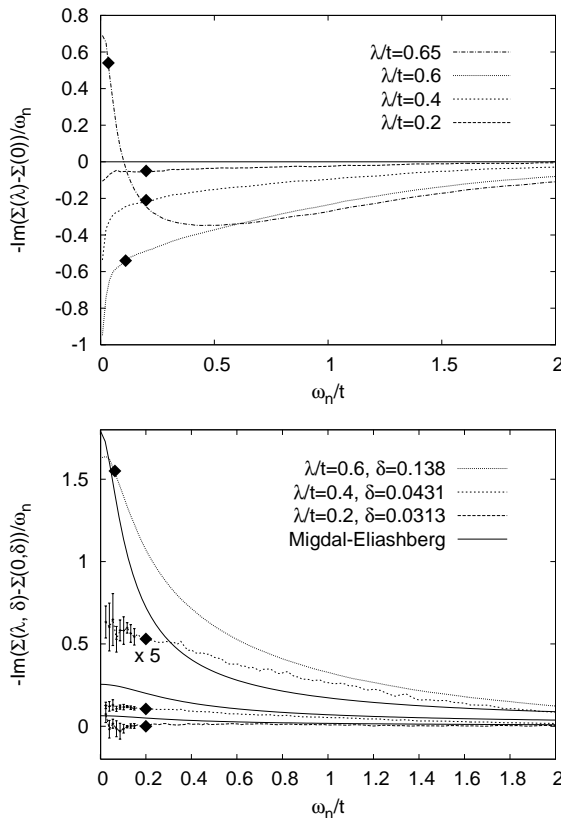


FIG. 3: Δr for several phonon coupling strengths ($\beta t = 400$). Upper panel: $U/t = 4$ and $n = 1$. Note that except for the largest coupling (very close to the bipolaronic phase) the phonon contribution has the opposite sign to that predicted by Eq. (8) and that there is no clear association between ω_0^{ren} (indicated by black diamonds) and the frequency scales relevant for the self energy. Lower panel: $U = 6t$ (above the critical value for Mott insulating behavior), with λ and dopings as shown. While the difference is positive, there is again no clear association between the frequency scale and ω_0^{ren} .

the effective mass. In the doped Mott insulator at weak coupling the phonon contribution is zero within errors; for stronger couplings the phonon contribution has a sign consistent with Migdal-Eliashberg theory, but a smaller magnitude and substantially different frequency dependence. In particular, we see that ω_0^{ren} does not correspond to the frequency scale characterizing changes in Σ . These results show that the Migdal approximation fails badly as the quasiparticle scale becomes comparable to the renormalized phonon frequency. Although the applicability of single-site DMFT to two dimensional materials is questionable, our results suggest that caution is required in interpreting data [1] in terms of a Migdal-Eliashberg picture.

To summarize: we have introduced a new method which enables simulations of models with electron-phonon coupling at essentially the same computational cost as simulation of models without phonons. We ap-

plied the result to the Holstein-Hubbard model, showing that for this case, the natural expectation [13], that a renormalized Migdal-Eliashberg theory applies, is simply wrong. In particular, the frequency dependence of the self energy is not directly related to the phonon frequency. We have presented results for the Holstein-Hubbard model, but the approach presented here generalizes straightforwardly to other models which can be solved by Lang-Firsov like transformations; for example to Jahn-Teller couplings in multiorbital models – although if pair-hopping terms are important one must perform a double-expansion in these and in the hybridization. Application of the method introduced here to models of manganites and to C_{60} (if the electronic spectrum is truncated to the 5 levels nearest the chemical potential) seems entirely feasible.

The calculations have been performed on the Hreidar beowulf cluster at ETH Zürich, using the ALPS-library [23]. We thank M. Troyer for the generous allocation of computer time, K. Ziegler for helpful discussions, and NSF-DMR-040135 for support.

- [1] A. Lanzara *et al.*, Nature **412**, 510 (2001).
- [2] O. Gunnarsson, Rev. Mod. Phys. **69**, 575 (1997).
- [3] M. Capone *et al.*, Science **296**, 2364 (2002).
- [4] A. J. Millis, P. B. Littlewood and B. I. Shraiman, Phys. Rev. Lett. **74**, 5144 (1995).
- [5] A. Yamasaki *et al.*, Phys. Rev. Lett. **96**, 166401 (2006).
- [6] J. K. Freericks, and G. D. Mahan, Phys. Rev. **B54**, 9372 (1996).
- [7] M. Tezuka, R. Arita, H. Aoki, Physica **B359**, 708 (2005).
- [8] Ju H. Kim *et al.*, Phys. Rev. **B 40**, 11378 (1989).
- [9] M. Grilli *et al.*, Nuc. Phys. **B744**, 277 (2000).
- [10] J. Bonca, T. Katracnik, and S. A. Trugman, Phys. Rev. Lett. **84**, 3153 (2000).
- [11] A. S. Mishchenko and N. Nagaosa Phys. Rev. Lett., **93**, 036402 (2004).
- [12] A. Georges *et al.*, Rev. Mod. Phys. **68**, 13 (1996).
- [13] A. Deppe and A. J. Millis, Phys. Rev. **B65**, 224301 (2002); Phys. Rev. **B65**, 100301 (2002); cond-mat/0204617.
- [14] W. Koller *et al.*, Europhys. Lett. **66**, 559 (2004);
- [15] M. Capone *et al.*, Phys. Rev. Lett. **92** 106401 (2004).
- [16] G. Sangiovanni *et al.*, Phys. Rev. Lett. **97**, 046404 (2006).
- [17] A. J. Millis, R. Mueller, and Boris I. Shraiman, Phys. Rev. **B54** 5389 (1996).
- [18] S. Blawid, A. Deppe, and A. J. Millis, Phys. Rev. **B67**, 165105 (2003).
- [19] P. Werner *et al.*, Phys. Rev. Lett. **97**, 076405 (2006).
- [20] P. Werner and A. J. Millis, Phys. Rev. **B74**, 155107 (2006).
- [21] E. Gull *et al.*, cond-mat/0609438.
- [22] I. G. Lang and Y. A. Firsov, Sov. Phys. JETP **16**, 1301 (1962).
- [23] M. Troyer *et al.*, Lecture Notes in Computer Science **1505**, 191 (1998); F. Alet *et al.*, J. Phys. Soc. Jpn. Suppl. **74**, 30 (2005); <http://alps.comp-phys.org/> .